Exciton spectroscopy in $Zn_{1-x}Cd_xSe/ZnSe$ quantum wells

R. Cingolani, P. Prete, D. Greco, P. V. Giugno, M. Lomascolo, R. Rinaldi, and L. Calcagnile
Dipartimento di Scienza dei Materiali, Università di Lecce, Via Arnesano, I-73100 Lecce, Italy

L. Vanzetti,† L. Sorba,‡ and A. Franciosi
Laboratorio Tecnologie Avanzate Superfici e Catalisi, Istituto Nazionale di Fisica della Materia, Area di Ricerca, Padriciano 99, Trieste, Italy

(Received 26 July 1994)

Systematic temperature-dependent studies of optical absorption and photoluminescence in $Zn_{1-x}Cd_xSe/ZnSe$ strained-layer multiple-quantum-well samples grown by molecular-beam epitaxy were used to evaluate the well-width dependence and the composition dependence of the major excitonic properties. Exciton binding energies calculated by means of a variational method were found in good agreement with the experimental values obtained from the analysis of the absorption line shapes. The well-width dependence of the excitonic eigenstates were well reproduced by envelope-function calculations that included the effect of pseudomorphic strain.

I. INTRODUCTION

Excitons in $Zn_{1-x}Cd_xSe/ZnSe$ multiple-quantum-well (MQW) heterostructures exhibit relatively high stability as compared to excitons in bulk semiconductors, due to the enhancement of the binding energy and the reduction of the exciton-phonon coupling caused by quantum confinement in wide-band-gap materials. Excitons are thus found to play an important role in many-body processes such as lasing and nonlinear absorption, often even at room temperature by virtue of their large screening threshold and strong thermal stability. For example, excitonic gain has been demonstrated in $Zn_{1-x}Cd_xSe/ZnSe$ quantum wells of thickness and composition such that the exciton binding energy was larger than the LO phonon energy ($E_b > \hbar\omega_{LO}$).[1] A detailed study of excitons in $Zn_{1-x}Cd_xSe/ZnSe$ MQW's is thus important to understand the optical properties of these wide gap heterostructures, also in view of their application to blue-green optoelectronic devices. Recently, there has been a few reports on the excitonic properties of this type of MQW's,[2–8] in which samples of different structure and composition were investigated by absorption,[2,3,7] photoluminescence, electroreflectance,[5] magnetotransmission,[6] and photocurrent.[8] The results of these works have demonstrated the enhancement of the exciton binding energy in narrow and deep quantum wells (high Cd content) and the reduction of the exciton-phonon coupling with increasing the confinement. Here, we extend these works by systematic absorption experiments in $Zn_{1-x}Cd_xSe/ZnSe$ MQW's as a function of temperature, well composition, and width, for well widths L_W ranging between 3 and 20 nm, and for Cd concentration in the wells ranging from $x=0.1$ to 0.26. The exciton binding energies and the excitonic eigenstates were obtained from the line shape analysis of the absorption spectra, and compared with the results of variational calculations and envelope-function calculations, respectively. Our results provide a comprehensive description of the main excitonic and electronic properties of $Zn_{1-x}Cd_xSe/ZnSe$ MQW's. Further, the comparison of the heavy-hole and light-hole transitions (with quantum numbers up to $n=4$) with the calculated confinement energies over a wide range of size and composition values, allowed us to identify a set of material parameters which can reproduce satisfactorily the energy trend of the electronic states in these quantum wells. The remarkable agreement between the data and the results of the calculations for ideal heterostructures emphasizes at the same time the level of understanding achieved for the well width and composition dependence of the excitonic states and the quality of the heterostructures. The work is organized as follows: in Sec. II, we describe the samples and the experimental details. In Sec. III, we outline the variational model used for the calculation of the exciton binding energies and give the details of the eigenstate calculations. In Sec. IV, we discuss the experimental spectra and their comparison to the theoretical results. Our conclusions are drawn in Sec. V.

II. EXPERIMENT

The MQW's were grown by solid source molecular-beam epitaxy (MBE) on GaAs(001) substrates in a facility described elsewhere[9] that includes separate MBE growth chambers for II-VI and III-V materials interconnected by ultrahigh-vacuum (UHV) transfer lines. After thermal removal of the native GaAs oxide, a 0.5 μm n-GaAs buffer layer was grown at 580 °C. The sample was then cooled under As flux, and transferred in UHV to the II-VI growth chamber, where a 1.5 μm ZnSe buffer layer was grown at 290 °C onto the GaAs(001)$c(4\times4)$ sub-

strate. Ten period $Zn_{1-x}Cd_xSe$/ZnSe MQW's were then grown at 250 °C with growth interruption of 30 sec at each interface. More detail on the growth procedures can be found in Ref. 10 and 11.

In what follows we will discuss results for three groups of samples, designed to selectively investigate the effect of well width and well depth on the excitonic states. The four samples in group *A* were comprised of ten period $Zn_{1-x}Cd_xSe$/ZnSe MQW's with $x=0.11$ and well widths $L_W=3$, 7, 11, and 20 nm, respectively. The four samples in group *B* were comprised of MQW's with $x=0.23$ and $L_W=3$, 7, 11, and 20 nm, respectively. The seven samples in group *C* were comprised of MQW's with $L_W=3$ nm and Cd content $x=0.10$, 0.11, 0.13, 0.16, 0.20, 0.23, and 0.26, respectively. The width of the ZnSe barrier layers was fixed in all cases at 20 nm.

The well parameters in the three groups of samples correspond to exciton properties spanning the range from bulklike (3D) behavior to the quasi-two-dimensional (2D) limit. Changes in composition x cause variations in the depth of the quantum well and in the value of the elastic strain within the $Zn_{1-x}Cd_xSe$ layers, which are all expected to be pseudomorphically strained to the ZnSe buffer. The combination of these compositional and configurational parameters permits a fine tuning of the excitonic properties of the $Zn_{1-x}Cd_xSe$ MQW's, which can be investigated by systematic optical and structural studies.

The samples investigated in this work were analyzed by high-resolution double-crystal x-ray diffraction, in order to test the crystalline quality and assess the structural and compositional parameters. The results of these experiments are beyond the scope of this paper and will be reported in a forthcoming paper.[12] Good coincidence between the measured and nominal parameters has been found in most samples.

For transmission measurements, the heterostructures were first glued to a sapphire plate and the GaAs substrate mechanically polished down to a thickness of about 80 μm. The samples were then masked with a photoresist leaving the substrate exposed through 100-μm-diameter windows, and the GaAs selectivity removed by wet chemical etching using a H_3PO_4:H_2O_2:H_2O solution at 30 °C followed by a H_2SO_4:H_2O_2:H_2O solution at 40 °C. Absorption spectra from the remaining self-supporting films, comprised of the $Zn_{1-x}Cd_xSe$ MQW and the ZnSe buffer, were obtained by focusing the mechanically chopped light of a tungsten halogen lamp onto the windows. The samples were mounted on the cold finger of a closed-cycle He cryostat, the temperature of which could be varied from 10 to 300 K. The transmitted beam was dispersed by a 0.85-m double monochromator and detected using a cooled GaAs photon counting. The overall spectral resolution of the measurements was always better than 0.5 meV.

Photoluminescence experiments were performed using the blue line (4579 Å) of an Ar^+ laser with power of the order of 10 mW on the sample, and the same cryostat and detection equipment. In this case, a photon counting mode acquisition was employed, with a spectral resolution of 0.2 meV.

III. DATA ANALYSIS METHOD AND MODELING

The experimental absorption spectra were analyzed to extract the energy position of the excitonic series, the exciton binding energy, and the thermal broadening of the ground level heavy-hole exciton. Excitonic absorption features were fitted to Gaussian line shapes, with linewidths mainly reflecting the inhomogeneous broadening of the states, i.e., statistical fluctuations in the ternary allow composition, strain, and layer thickness. We mention, for example, that in the investigated composition range a $\pm 1\%$ fluctuation in the Cd content of the alloy would result in a fluctuation of ± 11 meV in the energy gap.[13] The corresponding unintentional modulation of the quantum-well depth would cause *per se* a fluctuation of 1–3 meV in the quantization energies of the carriers in the well. The steplike continuum of the quantum-well density of states was simulated by a step function, convoluted with the same Gaussian broadening function used to reproduce the exciton absorption feature, and with the inclusion of the Coulomb enhancement factor at the band edge (Sommerfeld factor),[14] which is found to play a minor role in these II-VI materials. The energy separation between the Gaussian absorption feature and the broadened continuum edge was obtained from a best fit of the data, and provides a reasonable indication of the exciton binding energy. This simple criterion is justified by the lack of any feature associated with the 2*s* state of the exciton in our spectra, due to the unavoidable broadening induced by local inhomogeneities in the well.

The absolute positions of the excitonic Gaussian absorption features were compared with transition energies calculated from the predicted electron and hole confinement energies, taking into account exciton binding energy. The energies of the confined conduction and valence subbands of the $Zn_{1-x}Cd_xSe$/ZnSe quantum wells were evaluated in the envelope function approximation. We should mention that most of the required band parameters are not very well known for ZnSe, zinc-blende CdSe, and the related ternary alloys.[15] Many theoretical and experimental studies of excitons in $Zn_{1-x}Cd_xSe$/ZnSe MQW's have used quite different values for conduction- and valence-band effective masses, deformation potentials, and band offsets.[2–8,16,17] The parameters used in our calculations are listed in Table I. These were found to better reproduce quantitatively and qualitatively the experimental data obtained from the different sets of samples investigated in this work. A major problem in the eigenstate calculations is the interplay between the band offset expected for the bulk, unstrained materials and the effect of the tetragonal strain field on the band extrema in determining the actual total band discontinuities. Most recent reports suggest that in $Zn_{1-x}Cd_xSe$/ZnSe MQW's the conduction-band offset is larger than that valence-band offset, and ranges between 0.7 and 0.9 of the band-gap difference ΔE_g.[3,4,7,17] The shifts of the conduction (c), heavy-holes (HH), and light-holes (LH) band edges due to the hydrostatic and uniaxial deformation of the strained $Zn_{1-x}Cd_xSe$/ZnSe heterostructures are given by[18]

TABLE I. Parameters used in the calculations described in this paper.

	ZnSe	CdSe	$Zn_{0.89}Cd_{0.11}Se$	$Zn_{0.77}Cd_{0.23}Se$
E_g (eV)	2.821[a]	1.765[a]	2.6758[b]	2.5253[b]
V_e (eV)			0.1026[b]	0.2091[b]
V_h (eV)			0.0426[b]	0.0866[b]
m_e (m_0)	0.16[a]	0.13[a]	0.1567[c]	0.1531[c]
m_{HH} (m_0)	0.6[a]	0.45[a]	0.5835[c]	0.5655[c]
m_{LH} (m_0)	0.145[d]		0.145	0.145
ϵ	8.8[d]	9.3[d]	8.85[c]	8.91[c]
a (Å)	5.6676[a]	6.077[a]	5.7126[c]	5.7617[c]
C_{11} (N/m^2)	8.26×10^{10} [a]	6.67×10^{10} [a]	8.085×10^{10} [c]	7.8943×10^{10} [c]
C_{12} (N/m^2)	4.98×10^{10} [a]	4.63×10^{10} [a]	4.94×10^{10} [c]	4.899×10^{10} [c]
α (eV)			−3.365[e]	−3.314[e]
b (eV)	−1.2	−0.8	−1.156[c]	−1.108[c]
Δ (eV)	0.43[d]		0.43	0.43

[a]Reference 4.
[b]Taking into account the energy shift of the bands due to the strain.
[c]Evaluated by linear interpolation from the bulk ZnSe and CdSe parameters.
[d]Reference 15.
[e]$\alpha=-(C_{11}+2C_{12})/3(\partial E_g/\partial P)$, where the $(\partial E_g/\partial P)$ was taken after R. J. Thomas, H. R. Chandrasekhar, M. Chandrasekhar, N. Samarth, H. Luo, and J. Furdyna, Phys. Rev. B **45**, 9505 (1992).

$$\delta E_c = 2\alpha_c \left[\frac{C_{11}-C_{12}}{C_{11}}\right]\sigma$$

$$\delta E_{HH} = \left[-2\alpha_v \left[\frac{C_{11}-C_{12}}{C_{11}}\right] + b\left[\frac{C_{11}+2C_{12}}{C_{11}}\right]\right]\sigma$$

$$\delta E_{LH} = \left[-2\alpha_v \left[\frac{C_{11}-C_{12}}{C_{11}}\right] - \frac{1}{2}b\left[\frac{C_{11}+2C_{12}}{C_{11}}\right]\right]\sigma - \frac{\Delta}{2} + \frac{1}{2}\left\{\Delta^2 + \frac{9}{4}\left[2b\left[\frac{C_{11}+2C_{12}}{C_{11}}\right]\sigma\right]^2 - 2\left[b\left[\frac{C_{11}+2C_{12}}{C_{11}}\right]\sigma\right]\Delta\right\}^{1/2},$$

where α_c and α_v are the conduction- and valence-band hydrostatic deformation potentials, respectively, C_{ij} are the elastic constants, σ is the strain (compressive), b is the uniaxial deformation potential, and Δ the spin-orbit splitting. The problem is how to share the total deformation potential α between the conduction and valence bands ($\alpha=\alpha_c+\alpha_v$). Therefore, we performed several calculations for different values of the band offsets (in the $0.7-0.9\Delta E_g$ range) with (i) $\alpha_c=0$, (ii) $\alpha_c=2/3\alpha$, and (iii) $\alpha_c=\alpha$. The combination of parameters that was found to better reproduce our experimental results was a conduction-band offset equal to about $0.8\Delta E_g$ and $\alpha_c=2/3\alpha$, as discussed in Sec. IV.

The exciton binding energy was evaluated through a variational calculation. In the effective-mass approximation, the in-plane motion of the electron and hole is transformed into a center-of-mass motion of the exciton and in the relative motion of the constituent carriers. Neglecting the kinetic-energy term of the in-plane motion, the exciton Hamiltonian can be written as

$$H = \sum_{i=e,h}\left[-\frac{\hbar^2}{2m_i}\frac{\partial^2}{\partial z_i^2} + V_i(z_i)\right] - \frac{\hbar^2}{2\mu}\left[\frac{\partial^2}{\partial x^2}+\frac{\partial^2}{\partial y^2}\right] - \frac{e^2}{\epsilon\sqrt{\rho^2+(z_e-z_h)^2}}, \quad (1)$$

where m_e, m_h are the effective masses of the electron and hole, μ is the reduced exciton mass, z_e and z_h are the coordinates perpendicular to the plane of the layers for the electron and hole, ρ is the in-plane relative position given by $\rho=\sqrt{x^2+y^2}$, x and y are the relative coordinates of electrons and holes, ϵ is the dielectric constant, $V_e(z_e)$ and $V_h(z_h)$ are the actual confinement potentials for electrons and holes, respectively. The fact that different effective masses exist along the different directions in the Brillouin zone of the semiconductor was not included in the model. The lowest exciton energy was calculated variationally with a simple trial function,

$$\Psi(\rho,z_e,z_h)=\psi_e(z_e)\psi_h(z_h)\phi_{e-h}(\rho), \quad (2)$$

where $\psi_e(z_e)$ and $\psi_h(z_h)$ are the exact electron and hole wave functions in the finite quantum well, respectively. ϕ is the wave function of the in-plane radial motion, given by a $1S$ orbital,

$$\phi_{e-h}(\rho)=\left[\frac{2}{\pi\lambda^2}\right]^{1/2}\exp\left[-\frac{\rho}{\lambda}\right], \quad (3)$$

where λ is the trial parameter representing the radius of the exciton orbit. This separable trial function is strictly correct only for narrow well structures,[20,21] however, it can be used to obtain an estimate of the exciton binding energy also for wider wells, its limiting value being the bulk exciton Rydberg.

IV. RESULTS AND DISCUSSION

Representative low-temperature absorption spectra for selected $Zn_{1-x}Cd_xSe/ZnSe$ MQW's are shown in Fig. 1. The strong excitonic feature around 2.8 eV is due to the ZnSe barrier and buffer layer absorption. At lower energies all samples exhibit distinct excitonic peaks superimposed to the QW continuum. The quantum-size effect is clearly demonstrated by the blueshift of the absorption spectrum with decreasing well width. Furthermore, samples with higher Cd content show absorption spectra extended toward the green range, reflecting the increased depth of the quantum well. Narrow wells ($L_W=3$ nm) exhibit a single confined subband, as expected. The absorption spectra become more structured in the 20-nm-wide MQW's, where at least three electron subbands may be confined in the well. The photoluminescence spectra (dashed lines in Fig. 1) exhibit clear excitonic bands with typical Stokes shift ranging between 2 meV for wide wells with little Cd content, and 20 meV for the narrow wells with high Cd content. This indicates that the exciton localization at compositional or thickness fluctuations is more important in deep quantum wells.

The temperature dependence of the absorption spectra in the MQW's provides information on the thermal stability of excitons in these heterostructures. In Figs. 2(a)–2(b), we show absorption spectra in the 10–300-K temperature range for MQW's with $x=0.16$ and $L_W=3$ nm, and $x=0.11$ and $L_W=20$ nm, respectively. As already reported in Refs. 1, 2, and 3, deep quantum wells (high Cd content) have strongly confined excitons, with large binding energies and clear exciton features observed up to room temperature [see Fig. 2(a)]. On the contrary, shallow quantum wells (lower Cd content) do not exhibit room-temperature excitonic absorption [see Fig. 2(b)].

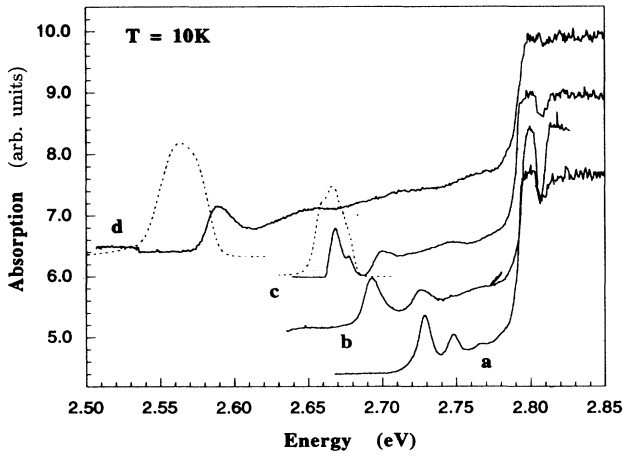

FIG. 1. (a) Absorption spectra of different $Zn_{1-x}Cd_xSe/ZnSe$ ten period multiple-quantum wells (MQW's) at 10 K. The sample parameters are $L_w=3$ nm, $x=0.11$ for sample (a), $L_w=3$ nm, $x=0.16$ for sample (b), $L_w=7$ nm, $x=0.11$ for sample (c), and $L_w=3$ nm, $x=0.23$ for sample (d). The dashed lines are the photoluminescence spectra recorded under low-power (10 mW) continuous wave excitation.

Exciton stability depends on the ratio of the exciton binding energy (E_b) to the LO-phonon energy ($\hbar\omega_{LO}=31.8$ meV in ZnSe), and on the actual strength of the exciton-phonon coupling. The latter parameter can be approxi-

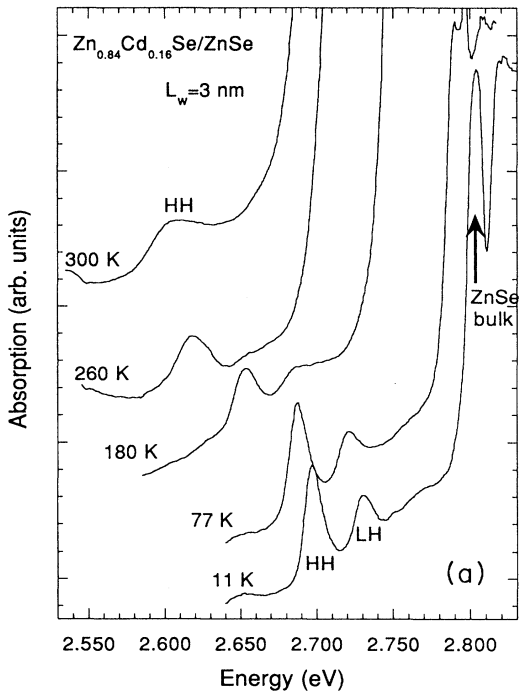

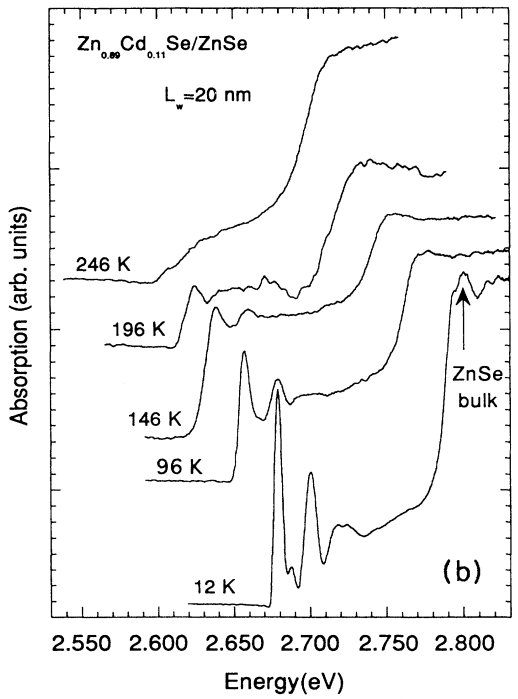

FIG. 2. (a) Temperature-dependence absorption spectra of a $Zn_{0.84}Cd_{0.16}Se/ZnSe$ MQW's sample with $L_W=3$ nm. (b) Temperature-dependence absorption spectra of a $Zn_{0.89}Cd_{0.11}Se/ZnSe$ MQW's sample $L_W=20$ nm.

mately estimated from the temperature-dependent absorption linewidth of the ground-level HH exciton, as obtained from the line-shape analysis of the experimental absorption spectra (Fig. 3). An example of the result of this line-shape analysis is shown in Fig. 3 for a $Zn_{0.84}Cd_{0.16}Se/ZnSe$ MQW with $L_W=3$ nm. The overall calculated absorption spectrum (solid line) obtained from a best fit to the data (solid circles) reproduces fairly well the experimental spectrum. The individual contributions of the heavy-hole (HH) and light-hole (LH) excitonic features and the HH interband continuum are also shown (dashed lines).

The exciton linewidth consists of an inhomogeneous term Γ_{inh}, due to composition and size fluctuations, and of a homogeneous term Γ_{LO}, due to lifetime broadening caused by the exciton-phonon interaction. The full width at half maximum (FWHM) of the exciton can be written as

$$\Gamma(T)=\Gamma_{inh}+\frac{\Gamma_{LO}}{\exp(\hbar\omega_{LO}/k_BT)-1} . \quad (4)$$

The inhomogeneous linewidth is temperature independent, and was derived from the absorption spectra measured at 10 K. The homogeneous term, proportional to the LO-phonon population, becomes important at high temperature. Analysis of the temperature-dependent absorption spectra from our samples by means of Eq. (4) (neglecting the contribution of acoustic-phonon scattering[6,22]) provides the Γ_{LO} values displayed in the inset of Fig. 3. Exciton-phonon coupling in narrow QW's (3 nm) is found to be smaller than in bulk ZnSe, whereas for wide wells (20 nm) it is larger than in the bulk, in agreement with recent experimental and theoretical work[7,6] for exciton-phonon coupling in $Zn_{0.75}Cd_{0.25}Se/ZnSe$ QW's. The reduced exciton-phonon coupling in narrow wells, is expected to favor exciton stability, in agreement with the results of Refs. 3, 4, and 7. We also observe in the inset of Fig. 3 that, for a given well width (3 nm), the exciton-phonon coupling appears to increase with increasing Cd content. This somewhat unexpected result[19] indicates that the increased exciton confinement occurring in deep $Zn_{1-x}Cd_xSe/ZnSe$ QW's would be partly balanced by the increased exciton-phonon coupling occurring in the Cd-rich alloy.

The systematic analysis of the low-temperature absorption spectra of the investigated samples provided the values of the ground level exciton binding energies. These are summarized in Fig. 4 for the different MQW's (solid circles and triangles for $x=0.11$ and 0.23 QW's, respectively), together with the results of the variational

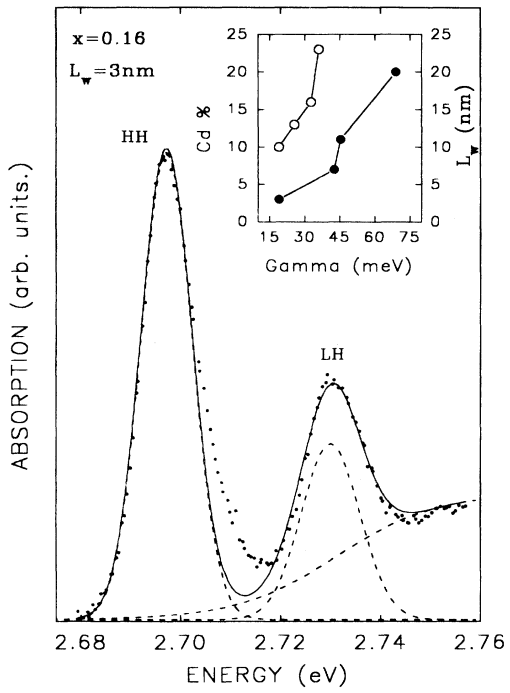

FIG. 3. Line-shape fit of an absorption spectrum at 10 K from a $Zn_{0.84}Cd_{0.16}Se/ZnSe$ MQW's sample with $L_W=3$ nm. The overall best fit (solid line) to the data (solid circles) is shown together with the individual heavy-hole (HH) and light-hole (LH) absorption features, and HH continuum (dashed lines). In the inset: exciton-phonon coupling constant (Γ_{LO}) from $Zn_{1-x}Cd_xSe/ZnSe$ MQW's versus well width L_W for $x=0.11$ (solid circles, right vertical scale) and versus Cd concentration x in the well (open circles, left vertical scale), as obtained from the temperature-dependent excitonic linewidth.

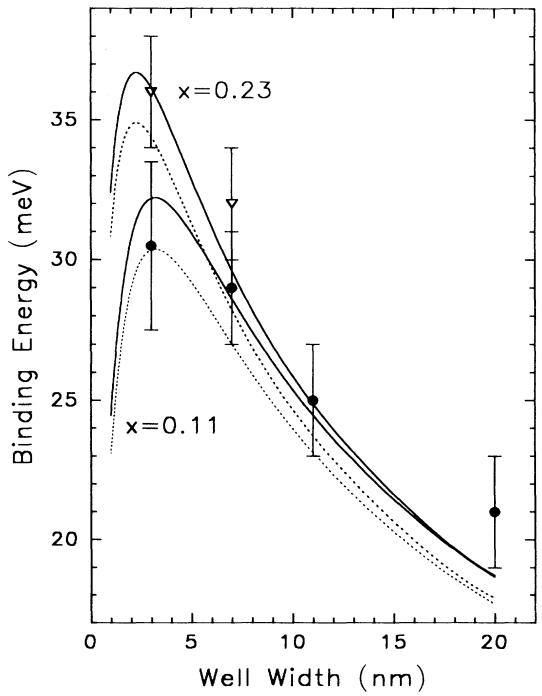

FIG. 4. Experimental exciton binding energy from 10 K absorption spectra for $Zn_{1-x}Cd_xSe/ZnSe$ MQW's with $x=0.11$ (solid circles) and $x=0.23$ (solid triangles) as a function of well width L_W. We also show the results of variational in calculations implemented using a linear interpolation of the dielectric constants [$\epsilon=8.8(1-x)+9.3x$ (solid curves) and $\epsilon=9.3$ (dotted lines)] and the band parameters in Table I.

calculations described in Sec. II (solid and dotted lines). For shallow MQW's, the calculated exciton binding energy varies from the bulk value (about 19 meV for $L_W=20$ nm) up to 32 meV for $L_W=3$ nm. For even lower well widths, the calculated exciton binding energy decreases, due to the increased penetration of the exciton wave function in the barriers. Deeper quantum wells ($x=0.23$) exhibit a similar behavior, but the maximum exciton energy is increased to about 37 meV for $L_W=2$ nm. The calculated values in Fig. 4 (solid and dotted lines) are in reasonable agreement with the data [symbols (Ref. 23)]. The only discrepancy is in the wide well region ($L_W=20$ nm), and is likely to reflect the limited accuracy of the trial wave function in Eq. (3) when the 3D exciton limit is approached.[20,21]

These results clearly show that exciton confinement in these $Zn_{1-x}Cd_xSe$/ZnSe MQW's can be tuned independently by varying the well composition or thickness. For example, an increase in exciton binding energy by a factor of two is obtained by decreasing L_W from 20 to 3 nm. On the other hand, for a given well width of 3 nm, an increase in the Cd content from $x=0.11$ to 0.26, i.e., an increase in well depth, results in a 15% enhancement of the exciton binding energy that reflects the enhanced localization of the carrier wave functions in the well. This is shown more clearly in Fig. 5, where we plot calculated (solid and dashed lines) and experimental (solid circles) ground-state exciton binding energies as a function of Cd content $0.1<x<0.26$ for a fixed well width $L_W=3$ nm (group C samples). The exciton binding energy is clearly seen to vary in Fig. 5 from just below to above the LO-phonon energy in the well-composition range examined.

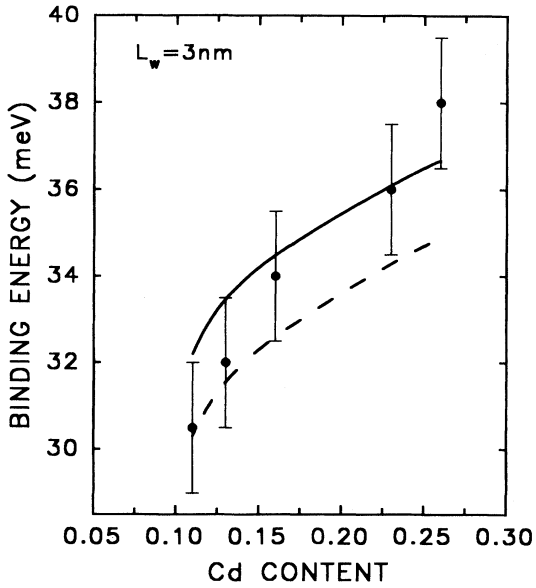

FIG. 5. Compositional dependence of the exciton binding energy in $Zn_{1-x}Cd_xSe$/ZnSe MQW's with $L_W=3$ nm and Cd concentration x spanning the 0.10–0.26 range, from absorption spectra at 10 K. We also show the results of variational calculations (solid and dotted lines) implemented as summarized in Fig. 4.

In this case, most of the binding-energy enhancement was found to derive from the relatively narrow well width (3 nm).

The data in Figs. 4 and 5 suggest that maximum exciton stability $E_b>\hbar\omega_{LO}$ cannot be achieved in shallow quantum wells ($x\simeq 0.1$). This is consistent with the observed thermal ionization of the exciton at room temperature and with the dominant free-carrier nature of the stimulated emission observed in our previous work on shallow MQW's.[24] Conversely, a strongly stabilized exciton exists in the deeper quantum wells investigated here ($x\simeq 0.2$), at least for sufficiently narrow well widths, as shown, for example, by the presence of a clear excitonic resonance in the room-temperature absorption spectrum in Fig. 2(a). Under these conditions, $E_b>\hbar\omega_{LO}$, and excitons may play an important role in the QW optical properties, including the recombination mechanism that accounts for stimulated emission in QW lasers in a wide range of injection levels and temperature.[1]

We have now all of the information required to evaluate the interband transition energies in the MQW's. In Fig. 6, we compare transition energies calculated in the envelope-function approximation including strain (see Sec. II) with the experimental values obtained by adding the binding-energy data in Fig. 4 to the experimental energy position of HH and LH features (solid and open cir-

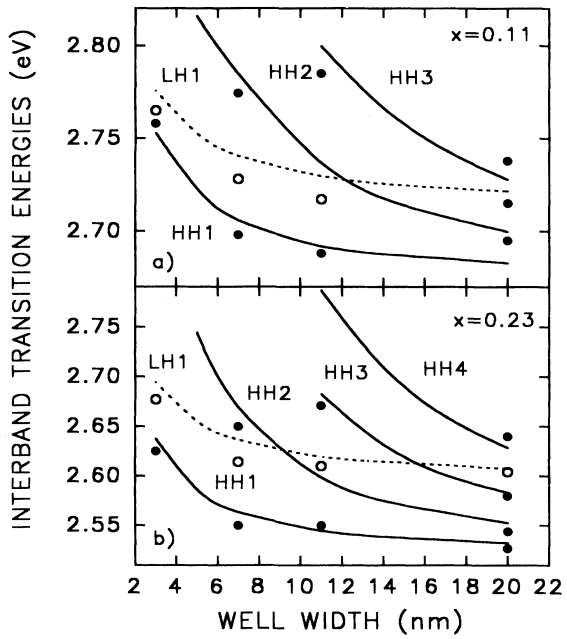

FIG. 6. (a) Interband HH (solid circles) and LH (open circles) transition energies for $Zn_{0.89}Cd_{0.11}Se$/ZnSe MQW's, as obtained from absorption spectra at 10 K. We also show the results of envelope-function calculations in the effective-mass approximation, including strain. The solid lines denote HH transitions of quantum number $n=1,2,3\ldots$. The dashed lines represent the LH transitions. The experimental values were obtained by adding the binding energy data in Fig. 4 to the experimental energy position of HH and LH features. (b) The same as in Fig. 6(a), but for $Zn_{0.77}Cd_{0.23}Se$/ZnSe MQW's.

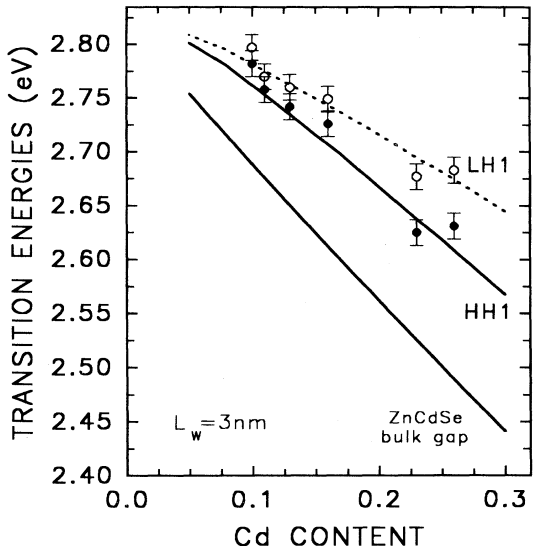

FIG. 7. Interband HH (solid circles) and LH (open circles) transition energies in $Zn_{1-x}Cd_xSe/ZnSe$ MQW's with $L_W=3$ nm, and x spanning the 0.10–0.26 range, from absorption spectra at 10 K. We also show the results of envelope-function calculations in the effective-mass approximation, including strain. The solid and dashed lines correspond to calculated HH and LH transitions, respectively. The experimental values were obtained by adding the binding-energy data in Fig. 5 to the experimental energy position of HH and LH features. A constant exciton binding energy of 20 meV was used for the LH transitions. The energy gap of the unstrained bulk ternary alloy $Zn_{1-x}Cd_xSe$ is also plotted for comparison (bottommost solid line).

cles in Fig. 6, respectively). We mention that in all of the investigated samples, the combination of strain and the relatively low-conduction-band discontinuity leads to a vanishing confinement potential for the LH states, largely independent of well width and composition. In particular, the depth of the LH potential well varies between 3 meV at $x=0.1$ and 15 meV at $x=0.3$, causing the light-hole states to be weakly confined or resonant with the continuum. This explains why the LH exciton features readily disappear from the absorption spectra with increasing temperature. In the calculations of Fig. 6, we have used the model of Ref. 25 for quantum wells of vanishing band offset, to evaluate a binding energy of about 20 meV for the LH exciton in $Zn_{1-x}Cd_xSe/ZnSe$ MQW's, irrespective of the well width and composition.

The calculated HH interband transitions with quantum number $n=1,2,3,\ldots$, (solid lines) and LH (dashed lines) in Fig. 6 are within 10 meV of the experimental values (solid and open circles), for both $Zn_{0.89}Cd_{0.11}Se/ZnSe$ (topmost section) and $Zn_{0.77}Cd_{0.23}Se/ZnSe$ MQW's. Such a difference is comparable to the experimental uncertainty expected for composition fluctuations of the order of $\pm 1\%$ in the well composition, and/or monolayer fluctuations in the well width for the narrow well width range (± 6 meV). Similar agreement is also found in Fig. 7, where we plot the Cd dependence of the ground level HH and LH excitonic transition energies for a series of MQW's with $L_W=3$ nm and well composition x spanning the 0.10–0.26 range (group C). The remarkable overall agreement between calculated and experimental exciton properties supports our choice of the band parameter in the model (see Table I) and our determination of the exciton binding energies. Different choices of band offset ratio and/or α_c and α_v would slightly worsen the agreement between calculated and experimental transition energies for the higher index excitonic eigenstates.

V. CONCLUSIONS

In conclusion, we have presented a systematic spectroscopic study of the excitonic states in $Zn_{1-x}Cd_xSe/ZnSe$ MQW's as a function of the well width and composition. The line-shape analysis of the temperature-dependent absorption spectra provided information on the thermal broadening of the ground level exciton, on the exciton binding energy and on the number of excitonic eigenstates in the different quantum wells. The data were compared with the results of variational calculations of the exciton binding energy and envelope-function calculations (including the strain) of the excitonic optical transition energies. We found that the excitonic parameters are strongly influenced by the well width, with a substantial increase of the exciton binding energy in narrow wells, and by the well composition, with a moderate enhancement of the exciton binding energy at higher Cd contents. Finally, good overall agreement between the calculated and measured series of excitonic eigenstates was found for different sets of samples, supporting the reliability of the band parameters used in the calculations and the exciton binding energies obtained from the absorption spectra.

ACKNOWLEDGMENTS

This work was supported in part by the U.S. Army Research Office under Grant No. DAAH04-93-G-0206, by INFM, and the Area di Ricerca. We thank P. Sciacovelli and L. Tapfer (CNRSM, Brindisi, Italy) for the x-ray-diffraction characterization of the samples and V. Pellegrini for useful discussions. The expert technical help of D. Cannoletta and G. Monteduro is gratefully acknowledged. Part of this work was sponsored by the Nova-Project of CNR-ITALY.

*Also with Istituto ICMAT del CNR, Montelibretti, Roma, Italy.

†Also with the Department of Chemical Engineering and Materials Science, University of Minnesota, Minneapolis, MN 55455 and Dipartimento di Fisica, Università di Trieste, Trieste, Italy.

[1] J. Ding, H. Jeon, T. Ishihara, M. Hagerott, A. V. Nurmikko, H. Luo, N. Samarth, and J. Furdyna, Phys. Rev. Lett. **69**, 1707 (1992); J. Ding, M. Hagerott, T. Ishihara, H. Jeon, and A. V. Nurmikko, Phys. Rev. B **47**, 10 528 (1993).

[2]J. Ding, N. Pelekanos, A. V. Nurmikko, H. Luo, N. Samarth, and J. K. Furdyna, Appl. Phys. Lett. **57**, 2885 (1990).

[3]N. T. Pelekanos, J. Ding, M. Hagerott, A. V. Nurmikko, H. Luo, N. Samarth, and J. K. Furdyna, Phys. Rev. B **45**, 6037 (1992).

[4]H. J. Lozykosky and V. K. Shastri, J. Appl. Phys. **69**, 3235 (1991).

[5]R. G. Alonso, C. Parks, A. Ramdas, H. Luo, N. Samarth, J. K. Furdyna, and L. R. Ram-Mohan, Phys. Rev. B **45**, 1181 (1992).

[6]N. T. Pelekanos, H. Haas, N. Magnea, H. Mariette, and A. Wasiela, Appl. Phys. Lett. **61**, 3154 (1992).

[7]P. M. Young, E. Runge, M. Ziegler, and H. Ehrenreich, Phys. Rev. B **49**, 7424 (1994).

[8]R. Cingolani, M. DiDio, M. Lomascolo, R. Rinaldi, P. Prete, L. Vasanelli, L. Vanzetti, F. Bassani, A. Bonanni, L. Sorba, and A. Franciosi, Phys. Rev. B **50**, 12 179 (1994).

[9]G. Bratina, G. Ceccone, A. Franciosi, M. Micovic, L. Sorba, F. Tommasini, and J. F. Walker, Vuoto (Italy) **20**, 565 (1990).

[10]L. Sorba, G. Bratina, A. Antonini, A. Franciosi, L. Tapfer, A. Migliori, and P. Merli, Phys. Rev. B **46**, 6834 (1992), and references therein.

[11]G. Bratina, L. Vanzetti, R. Nicolini, L. Sorba, X. Yu, A. Franciosi, G. Mula, and A. Mura, Physica **B185**, 557 (1993); G. Bratina, R. Nicolini, L. Sorba, L. Vanzetti, G. Mula, X. Yu, and A. Franciosi, J. Cryst. Growth **127**, 387 (1993).

[12]L. Tapfer, P. Sciacovelli, R. Cingolani, and A. Franciosi (unpublished).

[13]M. C. Tamargo, M. J. S. P. Brasil, R. E. Nahory, R. J. Martin, A. L. Waever, and H. L. Gilchrist, Semicond. Sci. Technol. **6**, 8 (1991).

[14]D. S. Chemla, D. A. B. Miller, P. W. Smith, A. C. Gossard, and W. Wiegmann, IEEE J. Quantum. Electron. **QE-20**, 265 (1984).

[15]H. E. Gumlich, D. Theis, D. Tschierse, in *Numerical Data and Functional Relationship in Science and Technology,* edited by O. Madelung, Landolt-Börnstein, New Series, Group III, Vol. 17, Pt. a (Springer, Berlin, 1982).

[16]Y. Kawakami, I. Hauksson, H. Stewart, J. Simpson, I. Galbraith, K. A. Prior, and B. C. Cavenett, Phys. Rev. B **48**, 11 994 (1993).

[17]H. Y. A. Chung, N. Uhle, and T. Tschudi, Appl. Phys. Lett. **63**, 1378 (1993).

[18]F. H. Pollak and M. Cardona, Phys. Rev. **172**, 816 (1968).

[19]This result seems to be in contrast with the expected reduction of the exciton-phonon coupling occurring in CdSe with respect to ZnSe. See, S. Rudin, T. L. Reinecke, and B. Segal, Phys. Rev. B **42**, 11 218 (1990).

[20]G. Bastard, E. E. Mendez, L. L. Chang, and L. Esaki, Phys. Rev. B **26**, 1974 (1982).

[21]D. A. B. Miller, D. S. Chemla, T. C. Damen, A. C. Gossard, W. Wiegmann, T. H. Wood, and C. A. Burrus, Phys. Rev. B **32**, 1043 (1985).

[22]J. Lee, E. Koteles, and M. O. Vassel, Phys. Rev. B **33**, 5512 (1986).

[23]The evaluation of the binding energy from the spectral separation between the exciton line and the continuum edge becomes very difficult in samples of high Cd content because of the strong alloy broadening. In the wider wells of group *B* the broadening becomes comparable to the subband splitting, and the interband continuum could not be resolved in the experimental spectra. Furthermore, the exciton binding energy measured and calculated in this work are larger than those obtained from the photocurrent spectra of Ref. 8. This discrepancy is probably due to the effect of the built-in electric field existing in the *p-i-n* structures investigated in Ref. 8.

[24]R. Cingolani, R. Rinaldi, L. Calcagnile, P. Prete, P. Sciacovelli, L. Tapfer, L. Vanzetti, G. Mula, F. Bassani, L. Sorba, and A. Franciosi, Phys. Rev. B **49**, 16 769 (1994).

[25]I. Galbraith, Phys. Rev. B **45**, 6950 (1992).